Induced coherence without induced emission

L. J. Wang, X. Y. Zou, and L. Mandel
Department of Physics and Astronomy, University of Rochester, Rochester, New York 14627
(Received 22 April 1991)

An interference experiment with signal and idler photons produced by parametric down-conversion in two nonlinear crystals is described and analyzed theoretically. It is found that when the idlers for the two crystals are superposed and aligned, the idler photon from the first crystal can induce coherence between the two signals, but without inducing any additional emission. Blocking the first idler wipes out the interference. The implications for the interpretation of the quantum state vector are discussed, and this leads to the conclusion that the state reflects not only what is known, but to some extent also what is knowable in principle.

PACS number(s): 42.50.Dv, 42.50.Kb, 42.65.Ky

I. INTRODUCTION

The idea that light produced by stimulated emission from some quantum source, like an atom, is coherent with the stimulating field has long been familiar. The same concepts are applicable to the process of down-conversion in a nonlinear crystal, in which incident pump photons interact parametrically with the medium and split into signal and idler photons [1–3]. It has been shown theoretically that the down-conversion can be stimulated by an external field and is coherent with the field [4], and this has been demonstrated in a recent experiment [5]. For this purpose the external field needs to be strong, i.e., it needs to have a large photon occupation number per mode. When the external field is weak, the down-conversion occur spontaneously and at random, and the spontaneously emitted light is then not expected to exhibit induced coherence.

Nevertheless, as has recently been demonstrated experimentally [6], it is possible to induce coherence in down-conversion without inducing emission. Such a situation occurs in the presence of two coherently pumped down-converters when the idler photon from the first down-converter passes through, and is aligned with, the idler from the second. It is then found that the two down-converted signals exhibit mutual coherence, and the degree of coherence between them can be controlled by varying the amplitude of the idler field reaching crystal No. 2 from crystal No. 1 [6]. The theory of this process was discussed only briefly in Ref. [6], where all fields were treated as monocrhomatic, whereas the down-converted photons are known to be in the form of very short wave packets [7]. In the following we present new experimental results for the interference between the two down-converted signals, particularly with respect to detection of signal and idler in coincidence. We also treat the process theoretically by the still approximate, but much more realistic, formalism that was introduced previously [8].

II. STATE OF THE FIELD

We refer to the experimental situation illustrated in Fig. 1 [6]. The two crystals NL1 and NL2 have $\chi^{(2)}$ nonlinear susceptibilities, and they are optically pumped by light beams derived from a common laser source of mid-frequency ω_0. We represent the pump beams at each crystal classically by the complex analytic signals $V_1(t)$ and $V_2(t)$ such that $|V_j(t)|^2$ is in units of photons per second ($j=1,2$). The interaction between the pump and the crystal generates down-converted signal (s) and idler (i) fields, which have to be treated quantum mechanically. In the interaction picture, we represent the parametric interaction between the pump field, the signal and idler fields, and the two crystals centered at $\mathbf{r}_1$ and $\mathbf{r}_2$ through the unitary time evolution operator in the form [6]

$$
\begin{aligned}
\hat{U}(t,t-t_1)&=\exp\left[\frac{1}{i\hbar}\int_{t-t_1}^{t}\hat{H}_I(t')dt'\right]\\
&=\exp\left\{\frac{(\delta\omega)^{3/2}}{(2\pi)^{1/2}}\eta_1\sum_{\omega_1}\sum_{\omega_1'}\sum_{\omega_1''}e^{i(\mathbf{k}_1-\mathbf{k}_1'-\mathbf{k}_1'')\cdot\mathbf{r}_1}\phi_1(\omega_1',\omega_1'';\omega_1)\frac{\sin(\omega_1'+\omega_1''-\omega_1)t_1/2}{(\omega_1'+\omega_1''-\omega_1)/2}\right.\\
&\qquad\times e^{i(\omega_1'+\omega_1''-\omega_1)(t-t_1/2)}v_1(\omega_1)\hat{a}^{\dagger}_{s_1}(\omega_1')\hat{a}^{\dagger}_{i_1}(\omega_1'')\\
&\quad+\frac{(\delta\omega)^{3/2}}{(2\pi)^{1/2}}\eta_2\sum_{\omega_2}\sum_{\omega_2'}\sum_{\omega_2''}e^{i(\mathbf{k}_2-\mathbf{k}_2'-\mathbf{k}_2'')\cdot\mathbf{r}_2}\phi_2(\omega_2',\omega_2'';\omega_2)\frac{\sin(\omega_2'+\omega_2''-\omega_2)t_1/2}{(\omega_2'+\omega_2''-\omega_2)/2}\\
&\qquad\left.\times e^{i(\omega_2'+\omega_2''-\omega_2)(t-t_1/2)}v_2(\omega_2)\hat{a}^{\dagger}_{s_2}(\omega_2')\hat{a}^{\dagger}_{i_2}(\omega_2'')-\text{H.c.}\right\}. \qquad (1)
\end{aligned}
$$

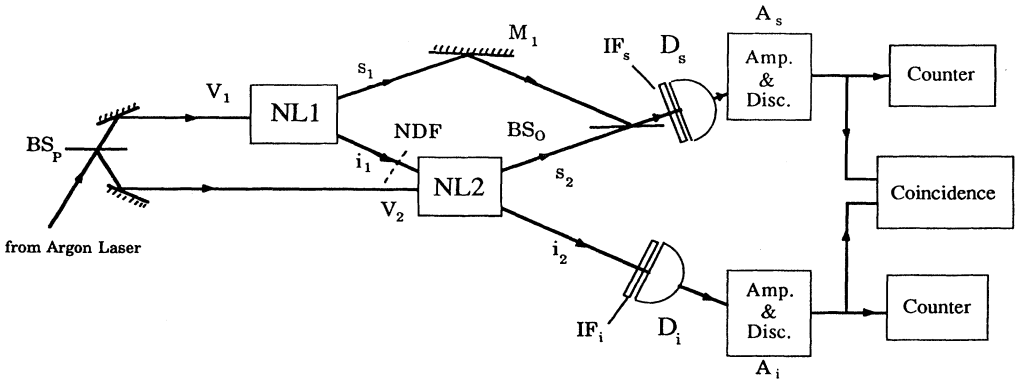

FIG. 1. Outline of the experiment.

Here t_1 is an interaction time that is much longer than the coherence time T_{DC} of the down-converted light. $\hat{a}_{s_j}^{\dagger}$ and $\hat{a}_{i_j}^{\dagger}$ are creation operators for signal photons and idler photons from crystal j. η_j is a constant such that $|\eta_j|^2$ gives the fraction of incident pump photons that is spontaneously down-converted in the steady state. $\delta\omega$ is the mode spacing, $\phi_j(\omega_j',\omega_j'';\omega_j)$ is a spectral function characterizing the signal and idler fields at crystal j, corresponding to a pump wave at frequency ω_j. $\phi_j(\omega_j',\omega_j'';\omega_j)$ is peaked at $\omega_j'=\omega_{sj}$, $\omega_j''=\omega_0-\omega_{sj}$, $\omega_j=\omega_0$ and is normalized so that ($\tilde{\omega}=\omega_0-\omega$)

$$2\pi\delta\omega\sum_{\omega}|\phi_j(\omega,\tilde{\omega};\omega_j)|^2=1\ . \tag{2a}$$

As $\delta\omega\to 0$ the sums over frequencies tend to integrals, and

$$2\pi\int_0^{\infty}d\omega|\phi_j(\omega,\tilde{\omega};\omega_j)|^2=1\ . \tag{2b}$$

In Eq. (1) it is taken for granted that the directions of the down-converted signal and idler fields characterized by $\mathbf{k}_j',\mathbf{k}_j''$ are well defined by apertures and can be regarded as fixed. One difference between the forms of the time evolution operators given in Eq. (1) and in Ref. [6] is that we have made Fourier decomposition of the pump fields by writing

$$V_j(t)=\left[\frac{\delta\omega}{2\pi}\right]^{1/2}\sum_{\omega_j}v_j(\omega_j)e^{i(\mathbf{k}_j\cdot\mathbf{r}_j-\omega_j t)}\ ,\quad j=1,2 \tag{3}$$

in order to allow for the possibility that certain path lengths in the interferometer may be comparable with the coherent time T_p of the pump field.

As is apparent from Fig. 1, the signal fields s_1 and s_2 from the two down-converters are allowed to come together and interfere at the detector D_s. The idler i_1 from crystal NL1 is aligned with the idler i_2 from NL2, passes through NL2 and falls on the detector D_i. In order to allow for the possibility that i_1 is attenuated by some filter before reaching NL2, we suppose that a 45° beam splitter BS_i has been inserted between NL1 and NL2 as shown, of amplitude transmissivity $\mathcal{T}$ and reflectivity $\mathcal{R}$ from one side and $\mathcal{T}',\mathcal{R}'$ from the other side. Then $\hat{a}_{i_2}(\omega)$ is related to $\hat{a}_{i_1}(\omega)$ via the usual equation

$$\hat{a}_{i_2}(\omega)=\mathcal{T}\hat{a}_{i_1}(\omega)+\mathcal{R}'\hat{a}_0(\omega)\ , \tag{4}$$

where $\hat{a}_0(\omega)$ describes the vacuum field entering at the unused input port of BS_i.

Let us assume that all quantum fields are in the vacuum state initially when the pump field is turned on. Then From Eqs. (1) and (4) the state of the field produced by both crystals at time t in the interaction picture is given by

$$\begin{aligned}|\psi(t)\rangle&=\hat{U}(t,t-t_1)|\psi_{\text{vac}}\rangle_{s_1,i_1,s_2,0}\\&=|\psi_{\text{vac}}\rangle_{s_1,i_1,s_2,0}+\eta_1\frac{\delta\omega^{3/2}}{(2\pi)^{1/2}}\sum_{\omega_1}\sum_{\omega_1'}\sum_{\omega_1''}\phi_1(\omega_1',\omega_1'';\omega_1)\frac{\sin(\omega_1'+\omega_1''-\omega_1)t_1/2}{(\omega_1'+\omega_1''-\omega_1)/2}\\&\quad\times e^{i(\omega_1'+\omega_1''-\omega_1)(t-t_1/2)}v_1(\omega_1)|\omega_1'\rangle_{s_1}|\omega_1''\rangle_{i_1}|\psi_{\text{vac}}\rangle_{s_2,0}\\&\quad+\eta_2\frac{\delta\omega^{3/2}}{(2\pi)^{1/2}}\sum_{\omega_2}\sum_{\omega_2'}\sum_{\omega_2''}e^{i(\mathbf{k}_2-\mathbf{k}_2'-\mathbf{k}_2'')\cdot\mathbf{r}_2}\phi_2(\omega_2',\omega_2'';\omega_2)\frac{\sin(\omega_2'+\omega_2''-\omega_2)t_1/2}{(\omega_2'+\omega_2''-\omega_2)/2}\\&\quad\times e^{i(\omega_2'+\omega_2''-\omega_2)(t-t_1/2)}v_2(\omega_2)|\omega_2'\rangle_{s_2}\\&\quad\times(\mathcal{T}^*|\omega_2''\rangle_{i_1}|\psi_{\text{vac}}\rangle_{s_1,0}+\mathcal{R}'^*|\omega_2''\rangle_0|\psi_{\text{vac}}\rangle_{s_1,i_1})+\cdots\end{aligned} \tag{5}$$

where the ellipsis represents terms with more than two photons. We have introduced the simplification of taking $\mathbf{r}_1$, the center of crystal NL1, to be the origin. So long as the interaction time t_1 is much shorter than the average time interval between down-conversions, we may neglect terms with more than two photons. Under these conditions the state corresponds to one produced by spontaneous down-conversion in NL1 and NL2.

III. RATES OF PHOTON DETECTION

Next we consider the electric fields $\hat{E}_s(t)$ and $\hat{E}_i(t)$ at the two detectors D_s and D_i. If τ_0, τ_1, τ_2, and τ_3 are the propagation times of i_1 from NL1 to NL2, of s_1 from NL1 to D_s, or s_2 from NL2 to D_s, and of i_2 from NL2 to D_i, we may write

$$\hat{E}_s^{(+)}(t)=\left[\frac{\delta\omega}{2\pi}\right]^{1/2}\frac{i}{\sqrt{2}}\sum_{\omega}\hat{a}_{s_1}(\omega)e^{-i\omega(t-\tau_1)}+\hat{a}_{s_2}(\omega)e^{i[\mathbf{k}_{s_2}\cdot\mathbf{r}_2-\omega(t-\tau_2)]}, \tag{6}$$

$$\hat{E}_i^{(+)}(t)=\left[\frac{\delta\omega}{2\pi}\right]^{1/2}\sum_{\omega}\hat{a}_{i_2}(\omega)e^{i[\mathbf{k}_{i_2}\cdot\mathbf{r}_2-\omega(t-\tau_3)]}. \tag{7}$$

The fields are all referred to the center of crystal NL1 as origin, and they are normalized so that $\hat{E}^{(-)}\hat{E}^{(+)}$, like $|V_j(t)|^2$, is in units of photons per second.

If the detectors D_s and D_i have quantum efficiencies α_s and α_i, respectively, then the average rates of photon counting are given by

$$R_s=\alpha_s\langle\psi(t)|\hat{E}_s^{(-)}(t)\hat{E}_s^{(+)}(t)|\psi(t)\rangle \tag{8}$$

and

$$R_i=\alpha_i\langle\psi(t)|\hat{E}_i^{(-)}(t)\hat{E}_i^{(+)}(t)|\psi(t)\rangle . \tag{9}$$

We then obtain with the help of Eqs. (5) and (6)

$$R_s=\alpha_s\left\langle\left|\frac{i}{\sqrt{2}}\eta_1\frac{(\delta\omega)^2}{(2\pi)}\sum_{\omega_1}\sum_{\omega_1'}\sum_{\omega_1''}\phi_1(\omega_1',\omega_1'';\omega_1)\frac{\sin(\omega_1'+\omega_1''-\omega_1)t_1/2}{(\omega_1'+\omega_1''-\omega_1)/2}\right.\right.$$

$$\times e^{i(\omega_1'+\omega_1''-\omega_1)(t-t_1/2)}e^{-i\omega_1'(t-\tau_1)}v_1(\omega_1)|\omega_1''\rangle_{i_1}|\psi_{\text{vac}}\rangle_{s_1,s_2,0}$$

$$+\eta_2\frac{(\delta\omega)^2}{2\pi}\sum_{\omega_2}\sum_{\omega_2'}\sum_{\omega_2''}e^{i[(\mathbf{k}_2-\mathbf{k}_2'')\cdot\mathbf{r}_2-\omega_2'(t-\tau_2)]}\phi_2(\omega_2',\omega_2'';\omega_2)\frac{\sin(\omega_2'+\omega_2''-\omega_2)t_1/2}{(\omega_2'+\omega_2''-\omega_2)/2}$$

$$\left.\left.\times e^{i(\omega_2'+\omega_2''-\omega_2)(t-t_1/2)}v_2(\omega_2)(\mathcal{T}^*|\omega_2''\rangle_{i_1}|\psi_{\text{vac}}\rangle_{s_1,s_2,0}+\mathcal{R}'^*|\omega_2''\rangle_0|\psi_{\text{vac}}\rangle_{s_1,s_2,i_1}|)\right|^2\right\rangle .$$

We now introduce the change of variables $\omega_1'+\omega_1''-\omega_1=\Omega_1$ and $\omega_2'+\omega_2''-\omega_2=\Omega_2$ in the first and second double sums, respectively. After replacing sums over ω_1' and ω_2' by integrals over Ω_1 and Ω_2, we have

$$R_s=\alpha_s\left\langle\left|\frac{i}{\sqrt{2}}\eta_1\delta\omega\sum_{\omega_1}\sum_{\omega_1''}\frac{1}{2\pi}\int d\Omega_1\phi_1(\omega_1-\omega_1''+\Omega_1,\omega_1'';\omega_1)\frac{\sin\Omega_1 t_1/2}{\Omega_1/2}e^{-i\Omega_1(t_1/2-\tau_1)}\right.\right.$$

$$\times e^{-i(\omega_1-\omega_1'')(t-\tau_1)}v_1(\omega_1)|\omega_1''\rangle_{i_1}|\psi_{\text{vac}}\rangle_{s_1,s_2,0}$$

$$+\eta_2\delta\omega\sum_{\omega_2}\sum_{\omega_2''}e^{i(\mathbf{k}_2-\mathbf{k}_2'')\cdot\mathbf{r}_2}\frac{1}{2\pi}\int d\Omega_2\phi_2(\omega_2-\omega_2''+\Omega_2;\omega_2)\frac{\sin\Omega_2 t_1/2}{\Omega_2/2}e^{-i\Omega_2(t_1/2-\tau_2)}$$

$$\left.\left.\times e^{-i(\omega_2-\omega_2'')(t-\tau_2)}v_2(\omega_2)(\mathcal{T}^*|\omega_2''\rangle_{i_1}|\psi_{\text{vac}}\rangle_{s_1,s_2,0}+\mathcal{R}'^*|\omega_2''\rangle_0|\psi_{\text{vac}}\rangle_{s_1,i_1,s_2})\right|^2\right\rangle . \tag{10}$$

If t_1 is much longer than the coherent time T_{DC}, or the reciprocal bandwidth $\Delta\omega$, of the down-converted light, which is generally very short, then the principal contributions to the Ω_1,Ω_2 integrals come from a range of Ω_1 and Ω_2 much smaller than $\Delta\omega$. Hence we may replace $\phi_1(\omega_1-\omega_1''+\Omega_1,\omega_1'';\omega_1)$ and $\phi_2(\omega_2-\omega_2''+\Omega_2,\omega_2'';\omega_2)$ by $\phi_1(\omega_1-\omega_1'',\omega_1'';\omega_1)$ and

$\phi_2(\omega_2-\omega_2'',\omega_2'';\omega_2)$ to a good approximation. The Ω_1,Ω_2 integrals then simplify and are well approximated by the standard Dirichlet integral

$$\frac{1}{2\pi}\int_{-\infty}^{\infty} d\Omega \frac{\sin\Omega t/2}{\Omega/2} e^{-i\Omega(t/2-T)}=1 \quad \text{if } T>0 , \tag{11}$$

and we obtain from Eq. (10)

$$R_S=\alpha_s \sum_{\omega''}\left[\left\langle\left|\frac{i}{\sqrt{2}}\eta_1\delta\omega\sum_{\omega_1}\phi_1(\omega_1-\omega'',\omega'';\omega_1)e^{-i(\omega_1-\omega'')(t-\tau_1)}v_1(\omega_1)\right.\right.\right.$$
$$\left.+\eta_2\delta\omega\sum_{\omega_2}\mathcal{T}^* e^{i(\mathbf{k}_2-\mathbf{k}_2'')\cdot\mathbf{r}_2}\phi_2(\omega_2-\omega'',\omega'';\omega_2)e^{-i(\omega_2-\omega'')(t-\tau_2)}v_2(\omega_2)\right|^2\Big\rangle$$
$$\left.+\left\langle\left|\mathcal{R}'^*\eta_2\delta\omega\sum_{\omega_2} e^{i(\mathbf{k}_2-\mathbf{k}_2'')\cdot\mathbf{r}_2}\phi_2(\omega_2-\omega'',\omega'';\omega_2)e^{-i(\omega_2-\omega'')(t-\tau_2)}v_2(\omega_2)\right|^2\right\rangle\right] .$$

Now the spectrum of the pump light is centered at ω_0 and its bandwidth is very much smaller than that of the down-converted light ($T_P \gg T_{\mathrm{DC}}$). Therefore we may replace $\phi_1(\omega_1-\omega'',\omega'';\omega_1)$ by $\phi_1(\omega_0-\omega'',\omega'';\omega_0)=\phi_1(\tilde{\omega}'',\omega'')$, and $\phi_2(\omega_2-\omega'',\omega'';\omega_2)$ by $\phi_2(\omega_0-\omega'',\omega'',\omega_0)=\phi_2(\tilde{\omega}'',\omega'')$ to a good approximation ($\tilde{\omega}=\omega_0-\omega$). Also for two similar nonlinear crystals we may put

$$\phi_1(\tilde{\omega},\omega)=\phi_2(\tilde{\omega},\omega)=\phi(\tilde{\omega},\omega) . \tag{12}$$

Finally, since the vector $\mathbf{k}_2''$ is parallel to $\mathbf{r}_2$ we may identify $\mathbf{k}_2''\cdot\mathbf{r}_2$ with $\omega''\tau_0$. Then with the help of Eqs. (2b) and (3) we obtain, since $|\mathcal{R}'|^2+|\mathcal{T}|^2=1$,

$$R_s=\tfrac{1}{2}\alpha_s[|\eta_1|^2\langle I_1(t-\tau_1)\rangle+|\eta_2|^2\langle I_2(t-\tau_2)\rangle$$
$$-i\eta_1^*\eta_2\langle V_1^*(t-\tau_1)V_2(t-\tau_2)\rangle$$
$$\times\mu(\tau_0+\tau_2-\tau_1)\mathcal{T}^* e^{-i\omega_i(\tau_0+\tau_2-\tau_1)}+\text{c.c.}] . \tag{13}$$

Here ω_s,ω_i are the center frequencies of the signal and idler, with $\omega_s+\omega_i=\omega_0$. We have introduced the normalized correlation function $\mu(\tau)$ of the down-converted light defined by

$$2\pi\int_0^{\omega_0} d\omega|\phi(\tilde{\omega},\omega)|^2 e^{-i\omega\tau}$$
$$=2\pi e^{-i\omega_i\tau}\int_{-\omega_i}^{\omega_s} d\omega'|\phi(\omega_s-\omega',\omega_i+\omega')|^2 e^{-i\omega'\tau}$$
$$\equiv e^{-i\omega_i\tau}\mu(\tau) . \tag{14}$$

$\mu(\tau)$ is normalized so that $\mu(0)=1$, and its range in τ is of order $\pm 1/\Delta\omega$. $I_1\equiv|V_1|^2$, $I_2\equiv|V_2|^2$ are the intensities of the two pump waves and they are time independent in a stationary field. We have identified the normalized second-order correlation function of the pump field

$$\frac{\langle V_1^*(t-\tau_1)V_2(t-\tau_2)\rangle}{\sqrt{\langle I_1\rangle\langle I_2\rangle}}\equiv\gamma_{12}(\tau_1-\tau_2) . \tag{15}$$

We note that according to Eq. (13) a steady state is reached for sufficiently long t_1 in which the rate R_s no longer depends on t_1.

Finally, let us suppose that τ_0,τ_2,τ_2 are incremented by small times $\delta\tau_0$, $\delta\tau_1$, $\delta\tau_2$, all of which are much shorter than the coherence time T_{DC} of the down-converted light. Then we may put

$$\gamma_{12}(\tau_1+\delta\tau_1-\tau_2-\delta\tau_2)\approx\gamma_{12}(\tau_1-\tau_2)e^{-i\omega_0(\delta\tau_1-\delta\tau_2)} . \tag{16}$$

With this approximate Eq. (13) reduces to

$$R_s=\tfrac{1}{2}\alpha_s\{|\eta_1|^2\langle I_1\rangle+|\eta_2|^2\langle I_2\rangle+2|\mathcal{T}||\eta_1\eta_2|\sqrt{\langle I_1\rangle\langle I_2\rangle}|\gamma_{12}(\tau_1-\tau_2)||\mu(\tau_0+\tau_2-\tau_1)|$$
$$\times\cos[\omega_i(\tau_0+\tau_2-\tau_1)+\omega_i\delta\tau_0+\omega_s(\delta\tau_1-\delta\tau_2)+\arg\eta_1\eta_2^*-\arg\gamma_{12}(\tau_1-\tau_2)-\arg\mu(\tau_0+\tau_2-\tau_1)-\arg\mathcal{T}_i-\pi/2]\} . \tag{17}$$

Hence the counting rate R_s exhibits interference as the path difference $c\delta\tau_0$ changes with periodicity $2\pi c/\omega_i$ and as $c(\delta\tau_1-\delta\tau_2)$ changes with periodicity $2\pi c/\omega_s$. The visibility $\mathcal{U}$ is given by

$$\mathcal{U}=\frac{2|\eta_1\eta_2|\sqrt{\langle I_1\rangle\langle I_2\rangle}|\gamma_{12}(\tau_1-\tau_2)||\mu(\tau_0+\tau_2-\tau_1)|}{|\eta_1|^2\langle I_1\rangle+|\eta_2|^2\langle I_2\rangle|}|\mathcal{T}| . \tag{18}$$

For maximum visibility $\tau_0+\tau_2$ and τ_1 should be equal to within T_{DC}, and $V_2(t-\tau_2)$ should equal $V_1(t-\tau_1)$. Then we may put $|\gamma_{12}(\tau_1-\tau_2)|=1$, $|\mu(\tau_0+\tau_2-\tau_1)|=1$, so that

$$\mathcal{V}=\left|\frac{2|\eta_1\eta_2|\sqrt{\langle I_1\rangle\langle I_2\rangle}}{|\eta_1|^2\langle I_1\rangle+|\eta_2|^2\langle I_2\rangle}\right||\mathcal{T}| . \tag{19}$$

The first factor has the familiar structure for interference fringes, although the intensities actually relate to the pump beams rather than to the two interfering beams. The factor $|\mathcal{T}|$ shows that the visibility is proportional to the amplitude transmissivity $|\mathcal{T}|$ of the beam splitter BS_i, and vanishes when $\mathcal{T}=0$. It follows that the idler i_1 passing through NL2 has induced coherence between the signals from the two down-converters.

IV. INDUCED DEGREE OF COHERENCE

The degree of coherence between the two signals s_1 and s_2 may be obtained in the usual way from the modulus of the normalized correlation function

$$\frac{\langle \hat{E}_{s_1}^{(-)}(t)\hat{E}_{s_2}^{(+)}(t)\rangle}{[\hat{E}_{s_1}^{(-)}(t)\hat{E}_{s_1}^{(+)}\rangle\langle\hat{E}_{s_2}^{(-)}(t)\hat{E}_{s_2}^{(+)}(t)\rangle]^{1/2}}\equiv\gamma_{s_1s_2} , \tag{20}$$

where $\hat{E}_{s_1}^{(+)}(t)$, $\hat{E}_{s_2}^{(+)}(t)$ stand for the first and second terms on the right side of Eq. (6), respectively. With the help of Eqs. (5) and (6) we then find by the same sort of argument as was used to derive Eq. (17), for the induced degree of coherence,

$$|\gamma_{s_1s_2}|=|\gamma_{12}(\tau_1-\tau_2)||\mu(\tau_1-\tau_2-\tau_0)||\mathcal{T}| . \tag{21}$$

Hence if $|\gamma_{12}(\tau_1-\tau_2)|=1$ and $|\tau_1-\tau_2-\tau_0|\ll 1/\Delta\omega$, the degree of coherence between the two signals s_1,s_2 is $|\mathcal{T}|$. In practice there may be some loss of coherence connected with the lack of complete correlation between the measured $\hat{E}_s^{(+)}$ and $\hat{E}_i^{(+)}$ fields. Nevertheless, the proportionality between $|\gamma_{s_1s_2}|$ and $|\mathcal{T}|$ is confirmed experimentally.

In order to show that the induced coherence is not accompanied by induced emission, we now calculate the photon emission rate from NL2 in the signal mode. If $\hat{E}_{s_2}^{(+)}$ is given by the second term on the right side of Eq. (6), we have

$$R_{s_2}=\tfrac{1}{2}\alpha_s\langle\psi(t)|\hat{E}_{s_2}^{(-)}(t)\hat{E}_{s_2}^{(+)}(t)|\psi(t)\rangle$$

$$=\tfrac{1}{2}\alpha_s\frac{(\delta\omega)^3}{2\pi}\left\langle\left|\eta_2\sum_{\omega_2}\sum_{\omega_2'}\sum_{\omega_2''}\phi_2(\omega_2',\omega_2'')\frac{\sin(\omega_2'+\omega_2''-\omega_2)t_1/2}{(\omega_2'+\omega_2''-\omega_2)/2}v_2(\omega_2)e^{i\mathbf{k}_{s_2}\cdot\mathbf{r}_2}e^{i(\omega_2'+\omega_2''-\omega_2)(t-t_1/2)}e^{-i\omega_2'(t-\tau_2)}e^{i(\mathbf{k}_2-\mathbf{k}_{s_2}-\mathbf{k}_{i_2})\cdot\mathbf{r}_2}\right.\right.$$

$$\left.\left.\times(\mathcal{T}^*|\omega_2''\rangle_{i1}|\psi_{\text{vac}}\rangle_{s_1,s_2,0}+\mathcal{R}'^*|\omega_2''\rangle_0|\psi_{\text{vac}}\rangle_{s_1,i_1,s_2})\right|^2\right\rangle . \tag{22}$$

The same argument that was used in the derivation of Eq. (17) then leads immediately to the steady-state result

$$R_{s_2}=\tfrac{1}{2}\alpha_s|\eta_2|^2\langle I_2\rangle(|\mathcal{T}|^2+|\mathcal{R}'|^2)=\tfrac{1}{2}\alpha_s|\eta_2|^2\langle I_2\rangle , \tag{23}$$

which is independent of $|\mathcal{T}|$ and describes the rate of spontaneous down-conversion from NL2, irrespective of what is happening at NL1. Similarly we may show that the rate of counting of D_i is given by

$$R_i=\alpha_i(|\mathcal{T}|^2|\eta_1|^2\langle I_1\rangle+|\eta_2|^2\langle I_2\rangle) , \tag{24}$$

which also corresponds to spontaneous emission from both crystals, Evidently the idler $i1$ does not induce down-conversion in crystal NL2 under the assumed conditions.

V. COINCIDENCE COUNTING

In order to calculate the rate of counting of the coincidence counter in Fig. 1 we first need to evaluate a two-time fourth-order correlation function. The probability amplitude for the transition from the initial state $|\psi(t)\rangle$ to the final state $|\Phi\rangle$ via two photon absorptions at times t and $t+\tau$ is of the form

$$\langle\Phi|\hat{E}_i^{(+)}(t+\tau)\hat{U}(t+\tau,t)\hat{E}_s^{(+)}(t)|\psi(t)\rangle .$$

If the time interval τ is much shorter than the average interval between down-conversions, then the possibility of additional down-conversions occurring within τ can be neglected. We may then approximate the $\hat{U}(t+\tau,t)$ operator by unity. After squaring and summing over final states we arrive at

$$\Gamma_{si}^{(2,2)}(\tau)=\langle\psi(t)|\hat{E}_s^{(-)}(t)\hat{E}_i^{(-)}(t+\tau)\hat{E}_i^{(+)}(t+\tau)\hat{E}_s^{(+)}(t)|\psi(t)\rangle . \tag{25}$$

With the help of Eqs. (5)–(7) we obtain

$$\Gamma_{si}^{(2,20)}(\tau)=\frac{1}{2}\left|\frac{(\delta\omega)^{5/2}}{(2\pi)^{3/2}}i\eta_1\mathcal{T}\sum_{\omega_1}\sum_{\omega_1'}\sum_{\omega_1''}\phi_1(\omega_1',\omega_1'';\omega_1)\frac{\sin(\omega_1'+\omega_1''-\omega_1)t_1/2}{(\omega_1'+\omega_1'')/2}e^{i(\omega_1'+\omega_1''-\omega_1)(t-t_1/2)}\right.$$
$$\times v_1(\omega_1)e^{-i\omega_1'(t-\tau_1)}e^{i[\mathbf{k}_1''\cdot\mathbf{r}_2-\omega_1''(t-\tau_3+\tau)]}$$
$$+\frac{(\delta\omega)^{5/2}}{(2\pi)^{3/2}}\eta_2\sum_{\omega_2}\sum_{\omega_2'}\sum_{\omega_2''}\phi_2(\omega_2';\omega_2'';\omega_2)\frac{\sin(\omega_2'+\omega_2''-\omega_2)t_1/2}{(\omega_2'+\omega_2''-\omega_2)/2}e^{i\mathbf{k}_2\cdot\mathbf{r}_2}$$
$$\left.\times e^{i(\omega_2'+\omega_2''-\omega_2)(t-t_1/2)}v_2(\omega_2)e^{-i\omega_2'(t-\tau_2)}e^{-i\omega_2''(t-\tau_3+\tau)}\right|^2. \tag{26}$$

We now use the same procedure as in Sec. IV to evaluate the sums. With the help of Eq. (11) we arrive at

$$\Gamma_{si}^{(2,2)}(\tau)=\tfrac{1}{2}\langle|i\eta_1\mathcal{T}V_1(t-\tau_1)g(\tau_1-\tau_3+\tau-\tau_0)e^{-i\omega_i(\tau_1-\tau_3+\tau-\tau_0)}+\eta_2V_2(t-\tau_2)g(\tau_2-\tau_3+\tau)e^{-i\omega_i(\tau_2-\tau_3+\tau)}|\rangle^2$$
$$=\tfrac{1}{2}[|\eta_1|^2|\mathcal{T}|^2\langle I_1(t-\tau_1)\rangle|g(\tau_1-\tau_3+\tau-\tau_0)|^2+|\eta_2|^2\langle I_2(t-\tau_2)\rangle|g(\tau_2-\tau_3+\tau)|^2$$
$$-i\eta_1^*\eta_2\langle V_1^*(t-\tau_1)V_2(t-\tau_2)\rangle\mathcal{T}^*g^*(\tau_1-\tau_3+\tau-\tau_0)g(\tau_2-\tau_3+\tau)e^{i\omega_i(\tau_1-\tau_2-\tau_0)}+\text{c.c.}], \tag{27}$$

where we have written

$$g(\tau)\equiv\int_{-\omega_1}^{\omega_s}d\omega\phi(\omega_s-\omega,\omega_i+\omega)e^{-i\omega\tau}. \tag{28}$$

Like the function $\mu(\tau)$ given by Eq. (14), $g(\tau)$ has a range in τ of order $1/\Delta\omega$, and it varies relatively slowly with τ (without oscillating at an optical frequency).

The final stage of the calculation is to integrate $\Gamma_{si}^{(2,2)}(\tau)$ with respect to τ over the resolving time T_R of the coincidence counter. We then arrive at the coincidence counting rate of the two detectors

$$R_{si}=\alpha_s\alpha_i\int_{-T_R/2}^{T_R/2}d\tau\Gamma_{si}^{(2,2)}(\tau). \tag{29}$$

In practice T_R greatly exceeds the range $1/\Delta\omega$, so that we are effectively integrating each term in Eq. (27) from $-\infty$ to ∞. With the help of Eqs. (14) and (28) we obtain

$$\int_{-T_R/2}^{T_R/2}d\tau g^*(\tau''+\tau)\approx\int_{-\infty}^{\infty}d\tau g^*(\tau'+\tau)g(\tau''+\tau)$$
$$=\int\int_{-\omega_i}^{\omega_s}d\omega'd\omega''\phi^*(\omega_s-\omega',\omega_i+\omega')\phi(\omega_s-\omega'',\omega_i+\omega'')e^{i(\omega'\tau'-\omega''\tau'')}\int_{-\infty}^{\infty}e^{i(\omega'-\omega'')\tau}d\tau$$
$$=2\pi\int_{-\omega_i}^{\omega_s}d\omega|\phi(\omega_s-\omega,\omega_i+\omega)|^2e^{-i\omega(\tau''-\tau')}$$
$$=\mu(\tau''-\tau') \tag{30}$$

When this is substituted in Eq. (27) and we increment $\tau_0,\tau_1,\tau_2,\tau_3$ by $\delta\tau_0,\delta\tau_1,\delta\tau_2,\delta\tau_3$ it yields the result

$$R_{si}=(\tfrac{1}{2})^2\alpha_s\alpha_i[|\eta_1|^2\langle I_1\rangle|\mathcal{T}|^2+|\eta_2|^2\langle I_2\rangle-i\eta_1^*\eta_2\sqrt{\langle I_1\rangle\langle I_2\rangle}\mathcal{T}^*\mu(\tau_2+\tau_0-\tau_1)$$
$$\times\gamma_{12}(\tau_1-\tau_2)e^{i\omega_i(\tau_1-\tau_2-\tau_0)}e^{-\omega_i\delta\tau_0}e^{-i\omega_s(\delta\tau_1-\delta\tau_2)}+\text{c.c.}]. \tag{31}$$

This exhibits interference with changing $\delta\tau_0$, $\delta\tau_1,\delta\tau_2$ with the same periodicities as does R_s given by Eq. (17). However, the visibility is given by

$$\mathcal{U}'=\frac{2|\eta_1\eta_2|\sqrt{\langle I_1\rangle\langle I_2\rangle}|\gamma_{12}(\tau_1-\tau_2)||\mu(\tau_2+\tau_0-\tau_1)|}{|\eta_1|^2\langle I_1\rangle|\mathcal{T}|^2+|\eta_2|^2\langle I_2\rangle}|\mathcal{T}|, \tag{32}$$

and this differs from $\mathcal{U}$ given by Eq. (18) by the appearance of the $|\mathcal{T}|^2$ factor in the denominator. Hence $\mathcal{U}'\geq\mathcal{U}$. In the special case $|\eta_1|^2\langle I_1\rangle=|\eta_2|^2\langle I_2\rangle$, $|\gamma_{12}(\tau_1-\tau_2)|=1=|\mu(\tau_2+\tau_0-\tau_1)|$, we have

$$\mathcal{U}'=\frac{2|\mathcal{T}|}{1+|\mathcal{T}|^2}. \tag{33}$$

VI. EXPERIMENT

The setup for the interference experiment is illustrated in Fig. 1. The two down-converters consist of two similar 25-mm-long nonlinear crystals of $LiIO_3$ (called NL1 and NL2), which are both pumped at right angles by the 351.1-mm line of an argon-ion laser. The laser beam is

divided into two at the pump beam splitter BS_P, which produces two pump beams of nearly equal intensities. The crystals are cut for type-I phase matching, and each is housed in a sealed quartz cell. Down-converted light beams at 632.8 nm are produced, denoted as idlers i_1, i_2 and also conjugate beams at 788.7 nm, which are referred to as signals s_1, s_2. The crystals are so aligned that i_1 from NL1 passes through NL2 and its trajectory coincides with i_2. The two superposed idlers fall on the photodetector D_i, as shown. The two signals s_1, s_2 are allowed to come together at the 50%:50% beam splitter BS_0, where they interfere and fall on photodetector D_s. Both detectors are cooled to $-20\,^{\circ}C$, and their photoelectric pulses, after amplification and shaping by the amplifier-discriminator combinations A_s, A_i, are counted by scalars. At the same time the pulses are fed to a coincidence counter having a 13-nsec resolving time (established in an auxiliary experiment) that registers simultaneous detections of signal and idler photons. Typical counting rates for D_i, D_s and for both detectors in coincidence are $R_i \simeq 5000$/sec, $R_s \simeq 400$/sec, and $R_{si} \simeq 4$/sec, respectively.

The output beam splitter BS_O is mounted on a movable stage, and is attached to the stage via a piezoelectric transducer that allows submicrometer displacements to be made. Larger displacements can be made with the help of a micrometer and stepping motor. The paths of the light beams are defined by apertures, and their bandwidths are determined by interference filters (IF) of 10^{12} Hz passband centered at 788.7 and 632.8 nm, respectively. This makes the coherence length of the down-converted light about $\frac{1}{3}$ mm, and all optical paths have to be balanced to this accuracy or better. Provision is made for inserting neutral density filters (NDF) between NL1 and NL2 of constant optical path length, but with various amplitude transmissivities $\mathcal{T}$.

The idlers are first aligned with the help of an auxiliary He:Ne laser beam, which is then turned off. It is necessary to equalize the paths from the beam splitter BS_P to NL2 directly and from BS_P to NL2 via NL1, to within the coherence length T_P of the multimode argon-ion pump laser. As the coherence length is of order 5 cm, this is relatively easy to do. The more difficult task is the equalization of the interferometer paths NL1 to mirror $M1$ to BS_O, and NL1 to NL2 to BS_O to within $\frac{1}{3}$ mm. This is accomplished by displacing BS_O successively in 50-μm steps until a fourth-order interference pattern of maximum visibility shows up in the coincidence counting rate R_{si}. Then the visibility of the second-order interference registered by D_s alone is also maximum.

VII. EXPERIMENTAL RESULTS

Figure 2 shows the results of measuring the coincidence counting rate R_{si} of detectors D_s and D_i, after subtraction of accidental counts, for various displacements of the beam splitter BS_O when the filter transmissivity $|\mathcal{T}| \approx 0.91$. The solid curve is the best-fitting sinusoidal function with the expected periodicity obtained by a least-squares-fitting procedure. The observed visibility is $\mathcal{U}' \approx 0.53 \pm 0.04$. Similar measurements were performed for five different values of $|\mathcal{T}|$ from 0 to 0.91. The results for the visibility $\mathcal{U}'$ as a function of $|\mathcal{T}|$ are plotted in Fig. 3. The solid curve is that expected from Eq. (32) with $|\gamma_{12}| = 1 = |\mu|$, when allowance is made for the different counting rates of detectors D_s and D_i. Although the uncertainties of $\mathcal{U}'$ are fairly large because of the rather low coincidence rates R_{si}, the results are nevertheless consistent with Eq. (32).

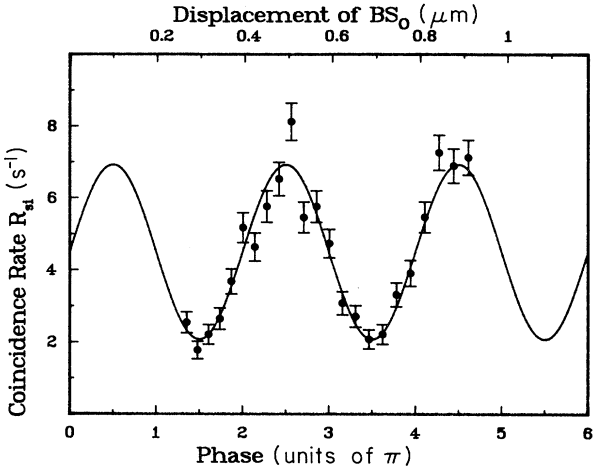

FIG. 2. Measured two-photon coincidence counting rate R_{si}, after subtraction of accidentals, as a function of BS_O displacement with filter transmissivity $|\mathcal{T}| = 0.91$. The solid curve is the best-fitting sinusoidal function of the expected periodicity. The error bars correspond to one standard deviation.

In Fig. 4 we plot the results of measuring the counting rate R_s of detector D_s alone as a function of BS_O displacement with $|\mathcal{T}| = 0.91$. The superposed curve A is

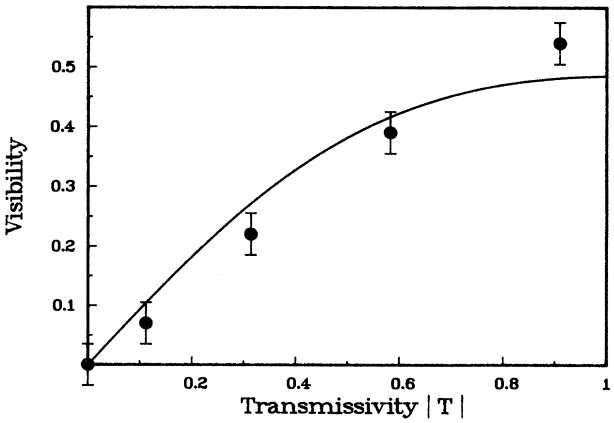

FIG. 3. Measured visibility $\mathcal{U}'$ of the interference registered by the coincidence counting rate R_{si} for various filter transmissivities $|\mathcal{T}|$. The solid curve is based on Eq. (32). Error bars show the statistical uncertainty.

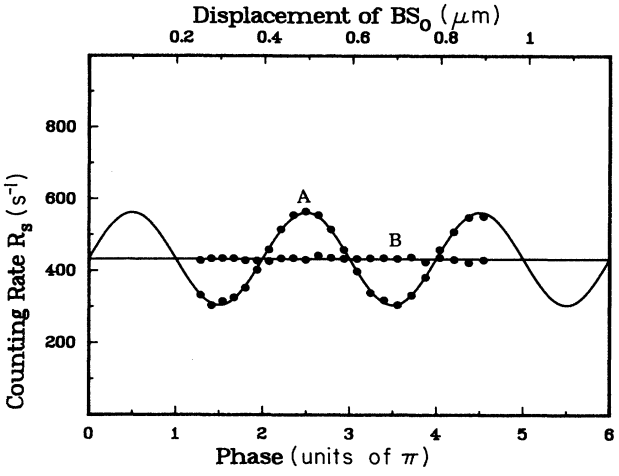

FIG. 4. Measured signal photon counting rate R_s as a function of BS$_O$ displacement. Curve A: $|\mathcal{T}|=0.91$; curve B: $|\mathcal{T}|=0$. The standard deviations are smaller than the dot size.

the expected sinusoidal function obtained by least-squares fitting. Because of the higher counting rate R_s compared with R_{si}, the standard deviations are now smaller than the dot size. The observed visibility $\mathcal{U}=0.3$ is smaller than $\mathcal{U}'$ under the same conditions, as expected from Eqs. (18) and (32). Curve B shows the results when the idler i_1 is blocked and cannot reach crystal NL2. In Fig. 5 we have plotted the measured visibilities $\mathcal{U}$ for various values of the filter transmissivity $|\mathcal{T}|$, superimposed on the straight line that is expected according to Eqs. (18) or (19). Once again the results are in reasonable agreement with the theory.

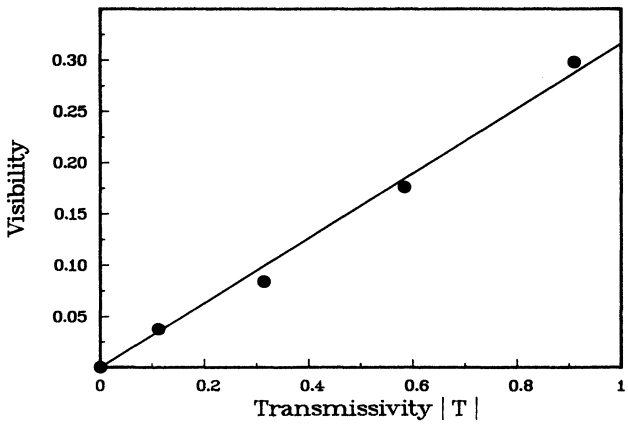

FIG. 5. Measured visibility $\mathcal{U}$ of the interference registered by the photon counting rate R_s for various filter transmissivities $|\mathcal{T}|$. The solid curve is based on Eq. (19) or (21). The statistical errors are smaller than the dot size.

VIII. DISCUSSION

Let us briefly discuss the implications of the experimental results as they relate to both the second-order and fourth-order measurements. It is not difficult to understand why the coincidence counting rate R_{si} exhibits interference when i_1 and i_2 are superimposed. In that case the signal and idler photon pair from either NL1 or NL2 can result in a coincidence detection. As these two outcomes are indistinguishable, one has to add the corresponding two-photon probability amplitudes for the two cases and then square to arrive at the probability. This leads to the observed fourth-order interference illustrated in Fig. 2. When i_1 is blocked and prevented from reaching NL2, a coincidence can only result from the signal and idler photon pair emitted by NL2 (apart from accidentals). There is therefore no ambiguity in what is observed and no interference. The situation is intermediate when $|\mathcal{T}|$ is neither close to unity nor zero.

Similarly, the counting rate R_s registered by D_s alone, when i_1 and i_2 are superimposed, exhibits interference. This may again be regarded as reflecting the intrinsic impossibility of knowing whether the detected photon comes from NL1 or NL2, and it also shows that i_1 is able to induce mutual second-order coherence between the signals s_1 and s_2 without causing any additional emission. This time it is, however, less obvious why the interference disappears when i_1 is blocked and prevented from reaching NL2. Because the down-conversions in both NL1 and NL2 are spontaneous, it might appear that detector D_s still has no way of knowing whether the detected photon comes from NL1 or NL2. Why then should the rate R_s not exhibit interference? The answer rests on a subtle point in the interpretation of the state vector (or density operator), for the state not only reflects what is known about the photon, but to some extent also what is knowable, in principle, under the given circumstances, whether it is actually known or not. If D_i is an efficient photodetector, it can be used, in principle, to determine whether a signal photon detected by D_s comes from NL1 or NL2 when i_1 is blocked. Whenever a detection by D_s is accompanied by a simultaneous detection by D_i, the signal photon must have come from NL2, and whenever a detection by D_s is not accompanied by a D_i detection, the signal photon must have come from NL1. It is the possibility of distinguishing between s_1 and s_2 that wipes out interference in the counting rate R_s, whether the auxiliary measurement with D_i is actually performed or not. This interpretational aspect of the interference effect is one of the more significant features of the experiment, besides the demonstration that induced emission need not always accompany induced coherence.

ACKNOWLEDGMENTS

We are indebted to Dr. Z. Y. Ou for the suggestion of aligning the two idlers, and to Mr. T. Grayson for help with the argon-ion laser. This work was supported by the National Science Foundation and by the U. S. Office of Naval Research.

[1] D. N. Klyshko, Zh. Eksp. Teor. Fiz. **55**, 1006 (1968) [Sov. Phys.—JETP **28**, 522 (1969)].
[2] B. Ya. Zel'dovich and D. N. Klyshko, Pis'ma Zh. Eksp. Teor. Fiz. **9**, 69 (1969) [JETP Lett. **9**, 40 (1969)].
[3] D. C. Burnham and D. L. Weinberg, Phys. Rev. Lett. **25**, 84 (1970).
[4] Z. Y. Ou, L. J. Wang, X. Y. Zou, and L. Mandel, Phys. Rev. A **41**, 1597 (1990).
[5] L. J. Wang, X. Y. Zou, and L. Mandel, J. Opt. Soc. Am. B **8**, 978 (1991).
[6] X. Y. Zou, L. J. Wang, and L. Mandel, Phys. Rev. Lett. **67**, 318 (1991); this paper contains the initial results of our experiment.
[7] C. K. Hong, Z. Y. Ou, and L. Mandel, Phys. Rev. Lett. **59**, 2044 (1987).
[8] Z. Y. Ou, L. J. Wang, and L. Mandel, Phys. Rev. A **40**, 1428 (1989).